Communications to SIMAI Congress,
ISSN 1827-9015, Vol. 1 (2006)
DOI: 10.1685/CSC06086

Modeling of Potential Fields by using Finite Element Method: The Etna Case Study

G. Currenti[(1)], C. Del Negro[(1)], L. Fortuna[(2)] and G. Ganci[(1, 2)]

(1) *Istituto Nazionale di Geofisica e Vulcanologia –Sezione Catania*
(2) *Università di Catania, Dipartimento di Ingegneria Elettrica, Elettronica e dei Sistemi*

Ground deformation and potential fields anomalies are important sets of observations for investigating the physic of the processes occurring at depth within the Mt. Etna volcanic edifice. During ascent, magma interacts with surroundings rocks and fluids, and almost inevitably crustal deformation and gravity changes are produced. If the volcanic edifice can be assumed to be elastic, contributions to gravity variations depend on surface and subsurface mass redistribution driven by dilation/contraction of the volcanic source. Attempts at modeling gravity anomalies expected to accompany crustal deformations often involve a great deal of effort due to the complexity of the problem. A series of analytical solutions for modeling coupled deformation-gravity variations due to volcanic sources have been devised and widely used in literature (Sasai, 1991; Okubo, 1992). Indeed, these analytical solutions are based on a homogeneous elastic half-space model, although geological data and seismic tomography indicate that the Mt. Etna is elastically inhomogeneous, and that rigidity layering and heterogeneities are likely to affect the magnitude and pattern of observed signals.

We use the finite-element method (FEM) to overcome these intrinsic limitations and provide more realistic models, which allows considering topographic effects as well as complicated distribution of medium properties. To this regard the gravity anomaly Δg produced by a pressurized source can be calculated by solving the following boundary value problem for the gravitational potential ϕ_g:

$$\begin{aligned} \nabla^2 \phi_g &= -4\pi G \Delta\rho(x,y,z) \\ \Delta g(x,y,z) &= -\left(\frac{\partial \phi_g}{\partial z}\right) \end{aligned} \tag{1}$$

where G is the gravitational constant and $\Delta\rho(x, y, z)$ is the density distribution given by:

$$\Delta\rho(x,y,z) = \delta\rho_1 - \rho_0 \, div\,\mathrm{u} - \mathrm{u}\cdot\nabla\rho_0 \tag{2}$$

The first term $\delta\rho_1$, on the right side of Eq. (2), is the density change related to the introduction of the new mass, the second term ρ_0 is the material density before deformation and is related to the contribution due to the volume change arising from compressibility of the material, the third term u is the displacement field and is originated from the displacement of density boundaries in heterogeneous media. The Eqs. (1) and (2) show how the deformations of the elastic medium are related to changes in the gravity fields. This formulation explains that gravity anomalies cannot be interpreted only in term of additional mass input disregarding the deformations of the surrounding rocks (Bonafede & Mazzanti, 1998).

Since displacement of layer boundaries can be computed independently from the assumption that new mass is added to the source or not, we consider source inflation/deflection without input of new magma, so the first term of Eq. (2) is equal to zero. Instead we focus our attention on the other two terms, the gravity anomaly produced by density changes within a semi-infinite medium (G4; Hagiwara, 1977) and the change (G2; Hagiwara, 1977) caused by the excess mass corresponding to uplift portion of the free surface (Bouguer anomaly) and the displacement of subsurface layers.

We reproduce our finite element model in two steps. Firstly, we solve the deformation field in terms of elastostatic equilibrium equations, calculating the displacement field and the stress field in over the computational domain. Then, we solve the boundary problem Eq. (1) for the coupled gravity

Licensed under the Creative Commons Attribution Noncommercial No Derivatives

potential. Computations are carried out by using the commercial software COMSOL Multiphysics, version 3.2.

FEM solutions strongly depend on numerical parameters. In general optimal size of the domain, meshing, and additional conditions to be imposed over the boundary are not known a priori, so it is necessary to calibrate the model. Preliminarily, some benchmark tests were carried out on the well-known solution of Mogi model to compare the analytical results with numerical ones assuming a homogeneous half-space medium. Once the accuracy of FEM solutions has been verified, we incorporate some realistic features in order to evaluate their effects.

We consider a 3D axial symmetric model, assuming an axial-symmetric shape of Etna volcano. For the sake of simplicity, we choose to model the gravitational effects caused by spherical pressurized Mogi sources: a dilation point buried at depth *d*, so the approximation with a sphere is valid until the radius *r* is little compared to the depth.

We consider three Mogi sources buried at 3 km, 6.5 km and 9 km, each one endowed with an internal overpressure equal to 100 MPa and a radius of 1 km. These parameters were chosen as commonly accredited for Etna volcano and could be interpreted as shallow magma reservoirs or deeper magma chambers.

For the deformation field calculation, computational domain is a 100x100 km^2 area. As boundary conditions we fix the displacement at the axis of symmetry in r-direction, while z-direction displacement is set to zero for the bottom, the extreme boundary at the distance of 100 km is fixed and the surface is stress free. As for the gravity calculation we solve the problem extending the computational domain up to an elevation of 100 km, in a way to assume the gravity potential equal to zero for the outermost boundaries, while Neumann conditions are imposed for the axis of symmetry.

At first we study the effects caused by the structural multi-layering of the medium. We retrieve density and elastic information about the crustal structure from the recent seismic tomography studies on Etna volcano (Chiarabba, 2000). Since the longitudinal wave velocities are directly linked to density (Birch, 1964) and other material parameters, such as elasticity, it is reasonable use seismic tomography information to refine our model.

As for the density values, also this information can be retrieved from tomography. Indeed in literature there exist several empirical relationships for seismic wave velocity and density depending on the subsurface geometry of geologic units and on chemical composition of the Earth's crust (Brocher, 2005). We retrieve a density model of the crust by using density-velocity relations (Crhistensen and Mooney, 1995; Gardner, 1974), interpolating these laws with a third order polynomial function that yields the following relationship:

$$\rho = 1.2861 + 0.5498Vp - 0.0930Vp^2 + 0.007Vp^3 \tag{3}$$

where ρ is the density and V_p is p-wave seismic velocity. Starting from p-wave velocities, we can obtain the medium elastic parameters. Particularly, we calculate the Young's modulus, E, through the relationship:

$$E = \frac{5}{6}\rho V_p^2 \tag{4}$$

assuming a Poisson ratio ν=0.25.

From these considerations, we introduce in the discussed model a multi-layered crustal structure described in Table 1. Since the deformation pattern is insensitive to the particular shape of interfaces between layers (Trasatti et al., 2003), we consider six horizontal layers characterized by different shear modulus and density.

Numerical solutions from finite element method were compared to analytical ones. For analytical half space solutions we consider an elastic medium with shear modulus equal to 25 GPa and density equal to 2500 kg/m^3. Fig. 1 shows the G4 and G2 gravity anomalies for the three sources for the multilayered model. For all the sources, the presence of density and elastic heterogeneities causes a modification of the gravity pattern. In the case of shallower reservoir (Figs. 1a and 1d), we notice an

increase in the amplitude of the signal about some tens of μGal. This effect decreases with the depth: for the source B, this amount assumes the order of some μGal (Figs. 1b and 1e) and for the deepest source (Fig. 1c and 1f) it becomes less than 1 μGal.

In order to appreciate a more realistic description, we choose to include in the numerical model a simple topographic profile assuming an axial-symmetric shape of Etna volcano. Since Mt. Etna, the largest stratovolcano in Europe, rises up to 3320 m above the sea level and its average radius is 20 km, we model the volcano edifice as a cone, introducing a simplified profile with an average slope of 15% where the sources are coaxial with the cone. We add this information to the heterogeneities and compare the gravity field anomalies with the analytical ones (Fig. 2). The presence of topography affects both the G2 and G4 gravity anomalies. The G2 term is attenuated for all the three sources (Figs. 2a, 2b, 2c), whereas the G4 term is dependent on the source depth (Figs. 2d, 2e, 2f). It is worth to note that the minimum amplitude in the G4 gravity anomaly is shifted some kilometers away from the summit. The distance of the local minimum from the summit increases for deeper sources. However the same effect is not detectable for G2 contribution in which only a change in its bell shape is detected. Topographic effects tend to decrease with increasing the horizontal distance from the summit.

Our findings highlight that topography and medium heterogeneity engender perturbations in the geophysical fields produced by a pressurized source. However, such perturbations are more enhanced in the presence of steepest topography, i.e. in the summit area, and in presence of severe heterogeneity. Whereas, further away from the summit the discrepancies between the analytical model and the numerical ones are less evident. Hence, neglecting the complexities associated with morphology and rheology of Mt. Etna could provide an inaccurate estimate of source parameters from geophysical observations. The inclusion of topography and structural heterogeneities might highlight significant insights for volcanic source definition.

Acknowledgement. This work was developed in the frame of the TecnoLab, the laboratory for the technological advance in geophysics organized by DIEES-UNICT and INGV-CT.

Bibliography

Birch, F.,;1964: Density and composition of mantle and core: J. Geophys. Res., 69(20) 4377-4388.

Bonafede, M. & Mazzanti, M.;1998: Modelling Gravity Variations Consistent with Ground Deformation in the Campi Flegrei Caldera (Italy), J. Volcanol Geotherm. Res. 81, 137–157.

Brocher, T.M.; 2005: Empirical Relations between Elastic Wavespeeds and Density in the Earth's Crust, Bull.Seism. Soc. America, 95, 2071-2092.

Chiarabba, C., A. Amato, E. Boschi, and F. Barberi; 2000: Recent seismicity and tomographic modeling of the Mount Etna plumbing system. J. Geophys. Res., 105(B5), 10,923–10,938.

Christensen, N. I. & Mooney ,W.D.;1995: Seismic velocity structure and composition of the continental crust: a global overview. J. Geophys. Res., 100(B2), 24,473–24,486.

Gardner, G.H.F., Gardner, L.W. & Gregory, A.M.; 1974: Formation velocity and density- the diagnostic basics for stratigraphic traps, Geophysics, 39(6), 770-780.

Hagiwara, Y.; 1977: The Mogi model as a possible cause of the crustal uplift in the eastern part of Izu Peninsula and related gravity change, Bull. Earthq. Res. Inst., Univ. Tokyo,52,301-309.

Okubo, S.;1992: Gravity and Potential Changes due to Shear and Tensile Faults in a Half-Space. J. Geophys. Res., 97(B5), 7137-7144.

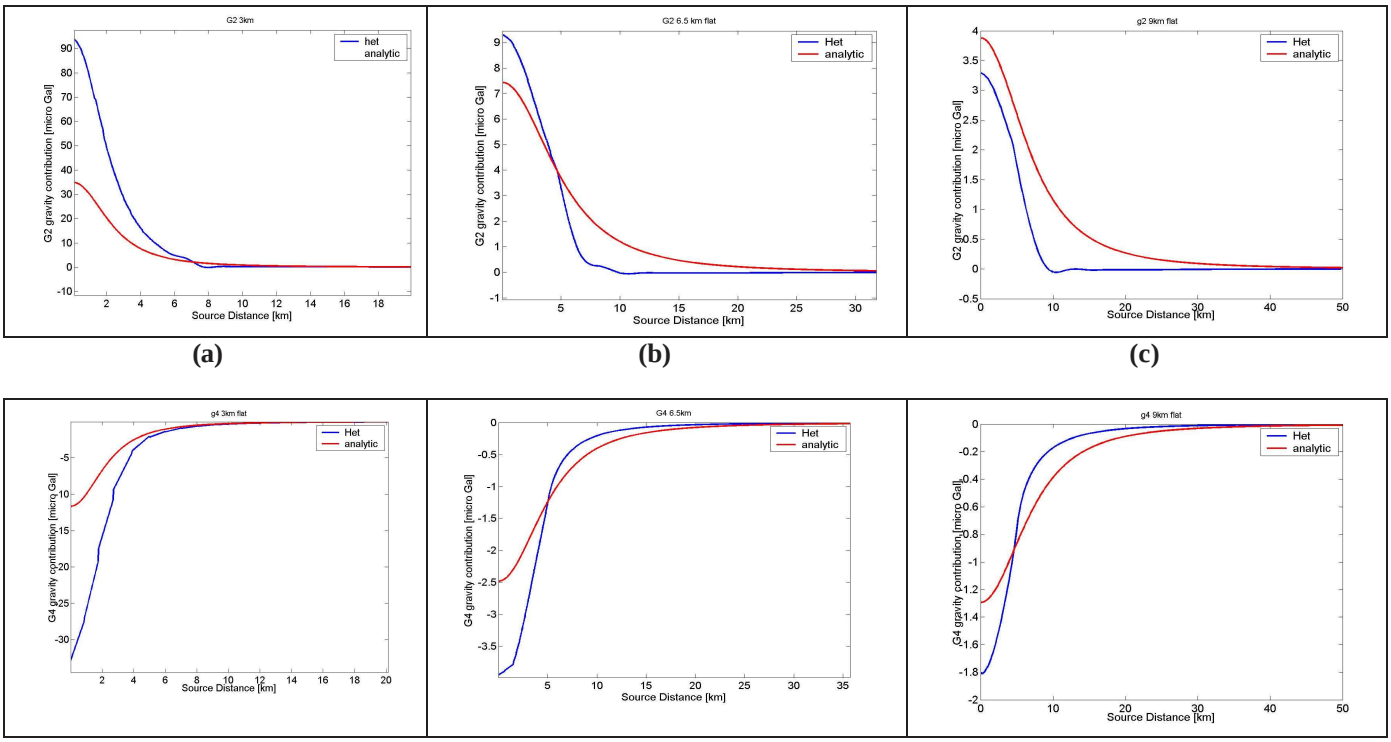
Sasai, Y.; 1991: Tectonomagnetic modeling on the basic of the linear piezomagnetic effect. Bull. Earthq. Res. Inst., Univ. Tokyo, 66, 585-722.

Trasatti, E., C. Giunchi, and M. Bonafede; 2003: Effects of topography and rheological layering on ground deformation in volcanic regions, J.Volcanol. Geotherm. Res., 122, 89–110.

Depth range [m]	Vp [m/s]	Density [kg/m^3]	Young Modulus [GPa]
3300 ÷ -1000	2.5	2200	11.5

-1000 ÷ -5000	3.8	2400	28.8
-5000 ÷ -8000	5.4	2600	63
-8000 ÷ -15000	6.2	2700	86
-15000 ÷ -23000	6.6	2800	101
-23000 ÷ -50000	7.3	3000	133

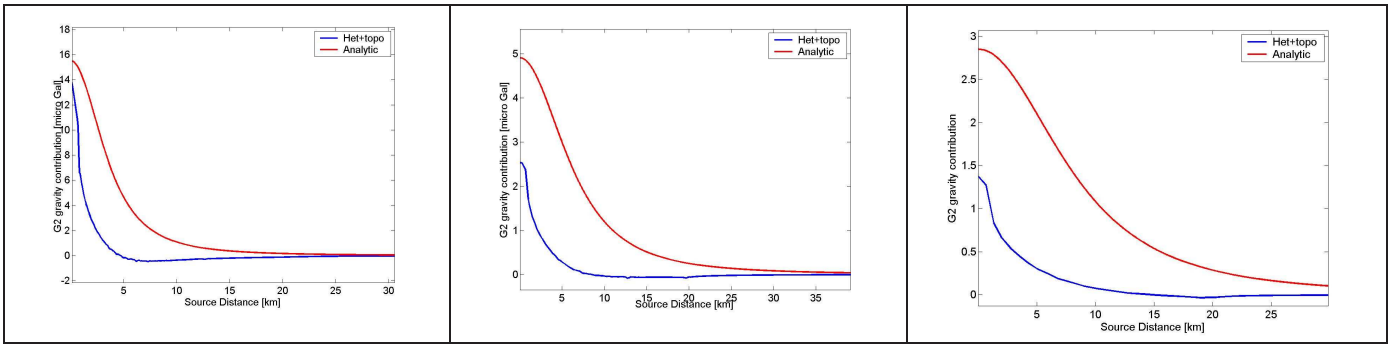
Table 1 - Multilayered crustal model



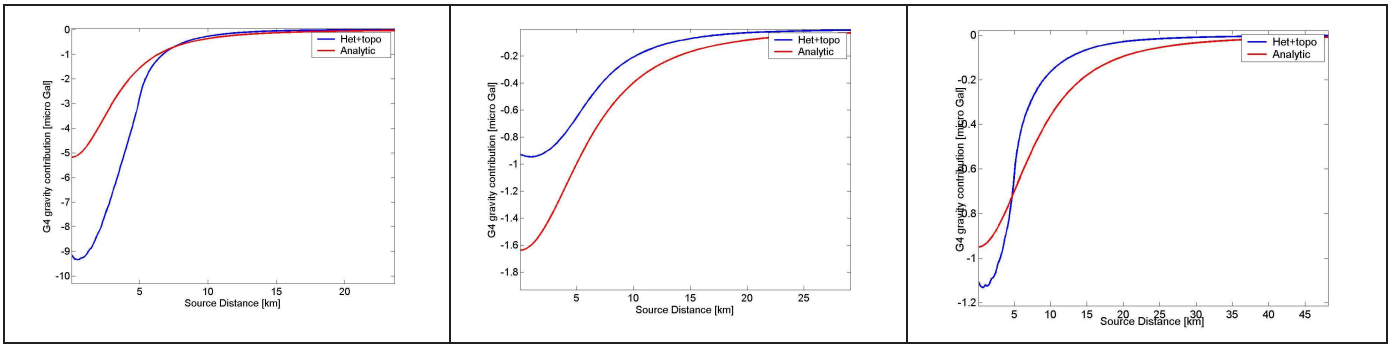
(a) **(b)** **(c)**

(d) **(e)** **(f)**

Figure 1 - Gravity contributions for the multilayered model.



(a) **(b)** **(c)**



(d) **(e)** **(f)**

Figure 2 - Gravity contributions in the heterogeneous medium (Table 1) with topography.